Published in final edited form as:
*Biomaterials*. 2007 June ; 28(18): 2830–2838.

# In vivo cellular repopulation of tubular elastin scaffolds mediated by basic fibroblast growth factor

**Aditee Kurane**, **Dan Simionescu**, and **Narendra Vyavahare***
*Department of Bioengineering, Clemson University*

## Abstract

*In vivo* tissue engineering has been explored as a method to repopulate scaffolds with autologous cells to create a functional, living, and non-immunogenic tissue substitute. In this study, we describe an approach to *in vivo* cellular repopulation of a tissue-derived tubular elastin scaffold. Pure elastin scaffolds were prepared from porcine carotid arteries (elastin tubes). Elastin tubes were filled with agarose gel containing basic fibroblast growth factor (bFGF) to allow sustained release of growth factor. These tubes were implanted in subdermal pouches in adult rats. The elastin tubes with growth factor had significantly more cell infiltration at 28 days than those without growth factor. Immunohistochemical staining indicated that most of these cells were fibroblasts, of which a few were activated fibroblasts (myofibroblasts). Microvasculature was also observed within the scaffolds. Macrophage infiltration was seen at 7 days, which diminished by 28 days of implantation. None of the elastin tubes with bFGF calcified. These results demonstrated that the sustained release of bFGF brings about repopulation of elastin scaffolds *in vivo* while inhibiting calcification. Results showing myofibroblast infiltration and vascularization are encouraging since such an *in vivo* implantation technique could be used for autologous cell repopulation of elastin scaffolds for vascular graft applications.

## Introduction

Cardiovascular diseases are the leading cause of death in the US. More than 500,000 bypass surgeries are performed annually [1]. Typically, autologous saphenous veins or internal mammary arteries are used for these procedures; however, limited availability has urged the need for synthetic replacements. In small diameter arterial replacements (<6mm), synthetic grafts often fail due to thrombosis-related occlusion. Tissue engineering of small diameter arteries has been the holy grail of research in the last decade. Since the overall goal is to mimic natural arteries, extracellular matrix (ECM) materials have been widely researched. Due to its abundance in the ECM, collagen is the most common matrix component utilized for vascular tissue engineering. On gelation, soluble collagen assembles into linear filaments which aggregate to form fibers. This fibrillar form is conducive to cell mediated remodeling and is remodeled over time as the cells lay down their own matrix [2]. However, these gels have inadequate mechanical properties to withstand hemodynamic pressures and shear stresses [3]. These collagen-based grafts also lack the elastin required to withstand continual pulsatile flow.

***Corresponding author:** Narendra Vyavahare, PhD, Cardiovascular Implant Research Laboratory, Department of Bioengineering, Clemson University, 401 Rhodes Engineering Research Center, Clemson, South Carolina, 29634; Phone: 864 656 5558; Fax: 864 656 4466, Email: narenv@clemson.edu.

Other materials being researched for vascular graft tissue engineering are decellularized arteries (porcine, canine, ovine) containing the native collagen and elastin networks [4–6]. Advantages of using decellularized xenogeneic arteries as vascular grafts include ready availability, ease of procurement from donors, and the preservation of the ECM which is important for strength and cell attachment [5]. However, cellular repopulation in decellularized arteries has been shown to be incomplete [7,8]. We hypothesized that this lack of cellular infiltration is related to the lower porosity of tissue due to dense collagen-elastin networks, and that the removal of collagen from the artery, in addition to cells, would increase the porosity of the scaffold. In our previous study, small square elastin scaffolds made from porcine aortic wall showed better in vivo repopulation compared to patches of decellularized aorta when implanted subdermally in rats [9].

In the present study, we wanted to test if small diameter tubular elastin scaffolds could be repopulated *in vivo*, in a rat subdermal implant model, for vascular graft applications. We also wanted to test if controlled release of bioactive molecules such as bFGF would enhance cellular infiltration in these scaffolds. The results demonstrated that the sustained release of bFGF brings about enhanced repopulation of elastin scaffolds while inhibiting calcification. Such an in vivo repopulation technique could be used as a minimally invasive method for autologous cell repopulation of elastin scaffolds for vascular grafts in bypass surgeries.

## Materials and methods

### Tubular scaffold preparation

Porcine carotid arteries (5–7mm diameter) were harvested at a local slaughterhouse, rinsed in cold phosphate buffered saline (PBS) and transported to the laboratory on ice. They were then cleaned of adherent tissue and fat and rinsed in cold PBS. Tissues were subsequently processed for the preparation of tubular elastin scaffolds, by cyanogen bromide (CNBr) treatment, to remove cells, collagen and other ECM components except elastic fibers [10]. Briefly, fresh tubular carotid artery samples were treated with 50 mg/ml CNBr (Acros Organics; Morris Plains, NJ) in 70% formic acid (Acros Organics; Morris Plains, NJ )(8 ml/cm$^2$) for 19 h at 20° C with gentle stirring, followed by 1 h at 60° C and boiling for 5 min to inactivate CNBr. The scaffolds were then stored in 70% ethanol as a disinfectant. This method produced pure elastin scaffolds (shown in previous publication [9]). For the subdermal implant study, samples were further washed in sterile saline.

### Preparation of bFGF loaded elastin tubes

Human recombinant basic fibroblast growth factor (bFGF, PeproTech Inc, Rocky Hill, NJ) was reconstituted in 5mM Tris buffered saline (TBS) (pH = 7.6) and diluted in the same buffer to a working concentration of 6.6 μg/ml. Agarose (MP Biomedicals; Solon, OH) solution (2%) was made in TBS, microwaved for 2 minutes to dissolve the agarose and maintained at 40°C on a heating plate. This solution was mixed with the working solution of bFGF in a 1:1 ratio to give a final agarose solution of 1% containing 3.3 μg/ml bFGF. For the experimental (EL-Gel-FGF group), 300 μl of this solution was pipetted into tubular elastin scaffolds. The agarose gel solidified immediately and then both sides of the scaffold were tied with a suture to keep the gel within the scaffold for the entire duration of implants. For the control (EL-Gel group), elastin tubes were filled with 1% agarose gel only. This entire procedure was done under sterile conditions. The scaffolds (n = 6 per group per time point) were prepared 1–2 hours before use and were stored in sterile conditions until implanted.

### In vitro bFGF release

To evaluate the sustained release of bFGF from agarose gel within the elastin scaffold, we prepared bFGF loaded tubes in the same way as described above. These samples were then

immersed separately in 1ml TBS (pH 7.6 containing sodium azide) in centrifuge tubes and gently shaken at 37°C for 28 days. Solutions were replaced at regular time points with fresh TBS. The quantity of bFGF released in solution was evaluated using a bFGF ELISA kit (Calbiochem; San Diego, California).

### Subdermal implantation of tubular elastin scaffolds

EL-Gel-FGF and EL-Gel samples were implanted subdermally (n = 6 per group per time point) in adult male Sprague Dawley CD rats weighing 250–300g, placed under general anesthesia, as described earlier [11]. Briefly, a 1 cm wide skin incision was made on the back of the rats, and two subcutaneous pouches were created in each rat by blunt dissection. One scaffold (~20 mm long, containing 300μl gel) was placed into each pouch and the incision closed with surgical staples. Animals were recovered and provided with food and water ad libitum. Upon recovery, analgesic (buprenorphine, 0.05 mg/kg, s.c.) was provided. After 7 and 28 days, animals were euthanized by $CO_2$ asphyxiation and the implants along with surrounding capsules were retrieved for analysis. The agarose gel was removed from all samples and stored separately.

### Histology

Explanted elastin tubes were rinsed with phosphate buffered saline (PBS), embedded in Tissue Tek OCT compound (Sakura Finetek, U.S.A. Inc., Torrance, CA), and frozen at −80°C. 6 μm thick sections were cut using a cryostat (Microm HM 505 N, Mikron Instruments, Inc.) and collected on glass slides. The samples were evaluated using hematoxylin and eosin (H&E) staining for general morphology and Gomori's one step trichrome (Gomori's) stain for matrix formation. Dahl's Alizarin stain was used for identifying calcium deposits. Verhoff-Van Gieson stain (VVG) was used to evaluate the integrity of elastic fibers. For explant analysis, digital pictures were taken from each section at 200X magnification and cell infiltration depth was measured using the Spot Advanced software (Diagnostic Instruments Inc., Sterling Heights, MI). Cells populated elastin scaffolds from outside in and thus infiltration depths were measured as the distance (in micrometers) between the innermost cellularized layer and the outer (abluminal) edge of the scaffold. Six measurements were taken from each slide for each implant. (n = 3 slides per group; 18 measurements per group)

### Immunohistochemistry

Cryosections (n = 3 per group) were immunostained using anti-rat prolyl-4-hydroxylase primary antibody (1:500 dilution) for fibroblasts (Sigma, St. Louis, MO), anti-rat macrophage (1:200 dilution) (Chemicon, Temecula, CA), anti-α-smooth muscle actin (1:200 dilution) for myofibroblasts (Sigma, St. Louis, MO) and anti-rat smooth muscle heavy chain myosin (1:3000 dilution) for smooth muscle cells. Vectastain Elite ABC Kit for mouse IgG and DAB substrate were used to visualize the specific staining (Vector Laboratories, Burlingame, CA). To minimize cross reactivity, rat-adsorbed biotinylated anti-mouse IgG at 5 mg/ml (Vector Laboratories) was used in place of the biotinylated secondary antibody provided with the staining kit. Negative controls were included with the omission of the primary antibodies. Sections were counterstained with hematoxylin.

### Protein extraction and analysis

Elastin scaffolds and gels (5 samples each) were separately weighed and homogenized on ice for two minutes in 300μl of extraction buffer (5mM TBS pH 7.6, 0.05% Triton X-100, 1mM proteinase inhibitor cocktail (Sigma Aldrich)). The homogenate was left on ice for 2 hrs after which it was ultracentrifuged (10,000 rpm, 20 minutes at 4°C). The supernatant was collected and analyzed for total protein content using BCA assay, bFGF content using an ELISA kit (Calbiochem) and matrix degrading enzymes such as MMPs using gelatin zymography.

### Mechanical testing

2–3 mm wide rings of fresh porcine carotid arteries, tubular elastin scaffolds (before implant, after 7 and 28 days of subdermal implantation) (n = 6 each) were subjected to radial tensile testing at a strain rate of 5 mm/s until failure on an MTS (Synergie 100) machine. Stress strain characteristics were plotted and the ultimate stress and engineering strain values were calculated. Young's modulus was calculated between 10 and 20% strain on the stress strain curve since this is the maximum strain usually experienced by arteries.

### Calcium assay

Quantitative analysis of calcium content in explanted scaffolds was performed according to a previously described procedure [12]. Briefly, a section of the capsule-free scaffold (n = 6 per group) was lyophilized, weighed and digested in 1ml of 6N HCl at 95 °C for 10 h. Digested samples were evaporated under a continuous stream of nitrogen gas until dry, and the residual material was dissolved in 1ml of 0.01N HCl. Calcium concentration was determined using an atomic absorption spectrophotometer (PerkinElmer, Norwalk, CT) and expressed as μg Ca/mg dry tissue.

### 2.10 DNA assay

Quantitative DNA analysis for the scaffolds was done using the DNeasy® tissue kit (Qiagen Inc. Valencia, CA). The protocol for DNA purification from rodent tails was used as described in the kit since the expected yield was 1 – 4μg DNA/mg wet tissue. Absorption was measured and the quantity of DNA calculated. Values are expressed as μg DNA/mg wet sample weight (n=6).

### 2.11 Statistical data analysis

Results are expressed as means ± standard error of the mean (SEM). Statistical analyses of the data were performed using single-factor analysis of variance (ANOVA). Subsequently, differences between means were determined using the least significant difference (LSD) with an alpha value of 0.05.

## Results

The purity of elastin scaffolds prepared by the CNBr treatment, evaluated by histology, SEM and other assays has been described in detail previously [13]. In the current study we attempted to repopulate tubular elastin scaffolds with cells by implanting them in a rat subdermal model. We developed an agarose gel system for the sustained delivery of bFGF within the scaffolds to improve cell infiltration.

### Release of bFGF from agarose gels

*In vitro* release studies of bFGF from 1% agarose gels showed a steady release of bFGF up to ~92% in 10 days (Figure 1A). Quantification of bFGF extracted from explanted scaffolds and gels showed that the growth factor was gradually released over 28 days from the agarose gel in the lumen and it moved into the elastin scaffold (Figure 1B). There was a 70% release from the gel in 7 days and a total 80% release in 28 days. Thus, *in vivo* release of bFGF correlated well with *in vitro* release.

### Cellular infiltration and neo-matrix deposition in subdermal implants

Macroscopically, the explants maintained their tubular structure and were covered by a very thin capsule that could be removed easily (Figure 2A and 2B). Agarose gels placed in the lumen were intact and could be removed easily. H&E staining showed that at 7 days there was almost no cellular infiltration in the EL-Gel group whereas there was a little infiltration in the EL-Gel-

FGF group (Figure 2C and 2D). At 28 days, EL-Gel showed similar infiltration as EL-Gel-FGF at 7 days whereas EL-Gel-FGF showed dense, organized infiltration halfway into the tissue (Figure 2E). Infiltration depth measurements (Table I) showed significantly higher infiltration at 28 days in the EL-Gel-FGF group (45.59% ± 1.98) as compared to all other groups. Gomori's trichrome staining (Figure 2F) for collagen showed organized collagen deposition within spaces between the sheets of the elastin only in the 28d EL-Gel-FGF scaffolds. There was hardly any collagen deposition in the remaining groups (data not shown) probably due to little cellular infiltration.

The majority of infiltrating cells in both groups at both time points were fibroblasts of which some stained positive for smooth muscle α-actin indicating their myofibroblastic phenotype (Figure 3A and 3B). Significant macrophage infiltration was observed at 7 days which reduced considerably at 28 days (Figure 3C and 3D). However, there were no smooth muscle cells as observed by the absence of smooth muscle heavy chain myosin staining (data not shown). Quantification of DNA (Figure 4) indicated twice as much DNA in the 28d EL-Gel-FGF group (0.3 ± 0.04 μg/mg) as compared to 28d EL-Gel as well as 7d EL-Gel-FGF (both ~ 0.16 ± 0.05 μg /mg). The value for 28d FGF group was statistically different from all other groups ($p < 0.05$).

### Changes in mechanical properties

Uniaxial radial tensile testing of rings of fresh porcine carotid arteries, elastin scaffolds (before implantation) and samples explanted at 7 and 28 days was done up to failure (Figure 5). Fresh carotid arteries showed typical biphasic characteristics with low modulus (150–200 kPa) up to ~ 50% strains and high modulus (3.5 – 4MPa) from 100 – 150% strain. The ultimate stress ranged from 1.76 – 2.64 MPa whereas the maximum strain ranged from 110% to 200%. Elastin scaffolds showed perfectly linear stress strain characteristics with a modulus ~400 kPa. The ultimate stress ranged between 0.42 and 0.85 MPa for strains between 80 – 140%. These characteristics are very much within the range of mechanical properties of pure elastin. [14] Both the EL-Gel and EL-Gel-FGF groups after 7 day subdermal implantation had exactly the same characteristics as the unimplanted elastin scaffold. However, after 28 days of implantation, both groups were stiffer with moduli ranging 1.3 – 1.65 MPa and had reduced elasticity. EL-Gel-FGF scaffolds could be strained upto ~80% whereas EL-Gel scaffolds were even less elastic and could only be strained upto ~50%. MMP-2 was detected in both groups at both 7 and 28 days whereas MMP-9 was detected in both groups only at day 7 (Figure 6A). Elastic fiber degradation was also seen on the outer (abluminal) side of the scaffolds (Figure 6B).

### Absence of calcification in subdermal implants

Calcification of implants was evaluated using quantitative calcium assay. None of the samples calcified in EL-Gel-FGF group (values ranged between 0 and 0.25 ± 0.1 μg/mg dry weight), while 2 out of 6 samples in the 28d EL-Gel group calcified significantly (8.1 and 15.8 μg/mg dry weight). Dahl's Alizarin staining of scaffolds did not show calcium deposits in EL-Gel-FGF group at both time points but there were a few spots in the EL-Gel group which was consistent with the quantitative studies (data not shown). The value for 28d EL-Gel group was statistically different from the 28d EL-Gel-FGF group ($p < 0.05$).

## Discussion

Tissue engineering of blood vessels has been focused on the search for the ideal material that will encourage regeneration to provide both a structural and functional replacement. The ideal vascular graft should be non-thrombogenic, non-antigenic, biodegradable and should have mechanical properties similar to the native artery (collagen for strength and elastin for recoil).

Most attempts to engineer small diameter blood vessels however, have failed clinically due to lack of one of the above characteristics. To eliminate immunorejection, a number of researchers have utilized the idea of *in vivo* tissue engineering of vascular grafts. Over 3 decades ago, Eiken [15], Schilling et al. [16,17], and most well known, Sparks, [18,19] first suggested the subcutaneous implantation of a mandril to allow a fibrocollagenous capsule to grow around it in 3–4 weeks. The mandril was removed and the tube that formed around it was used for vascular replacements. Though this method provided a completely autologous vessel, a follow up study by Hallin et al., [20] showed that the tubes occluded very quickly due to thrombus formation mainly due to the exposure of collagen fibers to blood. More recently, this idea of growing a blood vessel in the body was revived by Campbell et al., [21,22] when they implanted polymer tubing into the peritoneal and pleural cavities of animals to grow vessels similar to natural arteries. The collagenous capsule mainly contained myofibroblasts and was covered by a confluent layer of mesothelial cells. Before implantation as carotid interposition grafts in rabbits, the tubes were everted so that the mesothelium lined the lumen. This allowed the grafts to remain patent for at least 4 months. Although all these methods eliminated immunogenic problems (and later, thrombogenicity), two main questions arise. First, since the formation of a capsule is the body's way of sealing off a foreign body, these fibrocollagenous tubes that form in vivo are relatively avascular and thus may reduce exchange between cells and blood when implanted intravascularly. Second, these "biotubes" are rich only in collagen. Collagen provides tensile strength to arteries however, in order to sustain continual pulsatile flow and prevent dilatation (aneurysm formation), elastin is a necessary component [23]. Unfortunately, elastogenesis in tissue engineered constructs has been very limited [24], [25].

In the present studies we used porous elastin tubes carrying bFGF releasing gel for in vivo cellular repopulation. The bFGF releasing gel was contained within the lumen of the tubes by tying both edges of the tubular scaffold. This allowed cellular infiltration through only the abluminal side. The purpose of these studies was to provide intraluminal growth factor release to allow quicker abluminal cellular infiltration. On implanting these repopulated scaffolds into vasculature, elastin would provide the necessary elasticity to the graft.

The release of bFGF improved cell infiltration significantly. By 28 days, EL-Gel-FGF scaffolds were densely repopulated with host fibroblasts which synthesized new collagen within the elastic fiber network. Some of these fibroblasts showed a myofibroblast marker (smooth muscle α-actin) but were negative for smooth muscle heavy chain myosin staining (data not shown). These results are similar to those shown by others, who also showed a majority of myofibroblasts after implantation of 1 month [21,22,26]. These myofibroblastic cells have been shown to express strong smooth muscle cell markers under pulsatile flow either *in vitro* [27] or *in vivo* [22]. Thus, after implantation of such tubular scaffolds in the vasculature, myofibroblasts in the scaffolds may show SMC behavior.

Cellular infiltration within scaffolds in the EL-Gel-FGF group however, was incomplete and did not reach the intimal side, which could be advantageous for vascular applications for several reasons. First, adventitial fibroblast infiltration would mimic native adventitia and collagen deposition would provide adequate mechanical strength to the scaffold. Second, elastin will be exposed to the blood flow after vascular implantation which will minimize thrombus related failure. Tieche et al., [28] have shown that elastic laminae possess anti-thrombotic and anti-inflammatory properties and show significantly lower leukocyte adhesion when in contact with blood. Carr et al., [29] have also shown that elastin exhibits a four fold delay in clotting time when compared to synthetic biomaterials. Third, the space in the media that is not invaded by myofibroblasts during subdermal implantation could be infiltrated by smooth muscle cells laterally from the native artery after vascular implantation thus allowing a seamless interface with the native tissue.

We also observed microvasculature within the EL-Gel-FGF scaffolds. This observation is very important as cells need nutrients during neo-tissue development and many *in vitro* tissue engineering approaches fail due to inadequate nutrient supply deep within the scaffolds. Inadequate neovascularization of prosthetic vascular grafts often leads to infection, one of the most common causes of graft failure [30]. The observed microvasculature could be due to the release of bFGF, which is a well documented angiogenic growth factor [31,32].

One of the important aspects for vascular tissue engineering is appropriate mechanical strength of scaffolds prior to vascular implantation. We performed uniaxial tensile testing of rings of scaffolds after subdermal implantation to ensure that the scaffolds could still withstand physiological strains (arteries experience 1–4% strain and in extreme cases, 10% strain). [33]. The ultimate stress for the elastin scaffolds even before implantation is ~1/3$^{rd}$ that of fresh carotid arteries. This is due to the removal of collagen which provides tensile strength. After 7 days of subdermal implantation mechanical properties were comparable to the unimplanted elastin scaffolds This may be because there was very little cellular infiltration and little degradation of the scaffold. After 28 days of implantation, scaffolds from both groups became stiffer and less elastic. Synthesis of new collagen by infiltrating cells may be the cause of the increased stiffness whereas matrix degrading enzymes responsible for elastin remodeling may have reduced its elasticity. Moreover, though we tried to remove the fibrous capsule surrounding the elastin implant before mechanical tests were performed, there may have been some fibrous tissue remaining, which may account for the increase in stiffness in both EL-Gel and EL-Gel-FGF groups. EL-Gel scaffolds could be strained between 30 and 50% after 28 days whereas EL-Gel-FGF scaffolds could be strained between 50 and 80% before failure. Synthetic polymer scaffolds possess much lower ultimate strain even before implantation. Electrospun scaffolds composed of PLGA-elastin-collagen had a maximum strain of 40% at failure [34]. For the tissue engineering of blood vessels, burst pressure and compliance measurement are more important than static mechanical tests presented here. Although an extensive study was not performed to evaluate the burst pressure of the present scaffolds, water was pressurized through one EL-Gel-FGF scaffold after 28 days of implantation which burst at 300 mmHg. A wide range of burst pressures from 240 mmHg [35] to 650 mmHg [2] and in many cases in excess of 1000 mmHg [22,36] have been measured by different researchers. Native arteries have shown burst pressures between 2000 and 6000 mmHg depending on the animal and the vessel tested [37,38]. Detailed studies of burst pressure of EL scaffolds will be undertaken in the future.

An additional concern for vascular implants is pathologic calcification. We and others showed earlier that elastin based scaffolds are prone to calcification [39–41]. Cellular remnants are usually the nodes where calcification begins; however in some cases, even decellularization does not completely eliminate calcium deposition [42]. Attempts to alleviate elastin calcification have met with limited success even in adult rat models in which calcification is usually lesser than in juvenile animals[40,43].. In the present studies, interestingly, controlled release of bFGF suppressed elastin calcification while the control scaffolds without bFGF showed some calcification (statistically significant difference, $p < 0.05$). The role of bFGF in physiologic calcification is controversial. Some studies, mostly with bone, have shown that bFGF decreases mineralization by inducing hypophosphatemia [44]. The addition of bFGF to dentin pulp cultures suppressed the increases in ALPase activity, SPARC synthesis, and their mRNA levels [45]. However, other studies have shown that bFGF is associated with osteogenic properties especially when used in combination with bone forming proteins such as BMPs [46,47]. Our present studies, however, are the first to show suppression of elastin calcification by bFGF at 28 days in subdermal implantation model; however, whether this holds true for long-term studies and in the circulatory environment is unknown and needs further study in the future.

We have extensively studied mechanisms of elastin calcification and have shown that matrix degrading enzymes such as MMPs are involved in elastin calcification [12,48]. In this study, an initial inflammatory response (macrophage infiltration) seen at 7 days was reduced by 28 days. Macrophages were present in the surrounding capsule even at 28 days and MMPs were present in the scaffold (as seen by zymography). This led to some elastic fiber degradation on the outer edges of the scaffolds, but in EL-Gel-FGF scaffolds such MMP activity did not cause calcification. The mechanisms by which bFGF prevented elastin calcification in the rat subdermal implantation model would need further investigation.

## Conclusions

Subdermal implantation of elastin tubes loaded with bFGF releasing agarose gel provided a sustained release of growth factor which improved cell infiltration while preventing calcification of elastin. Although comprehensive mechanical testing of the scaffolds is required before implantation into the vascular system, this method provides a minimally invasive technique to prepare mechanically sound, autologous grafts that can be used as vascular replacements.

## References


1. Association, AH. Biostatistical factsheet: cardiovascular procedures. American Heart Association; 2003.
2. Berglund JD, Mohseni MM, Nerem RM, Sambanis A. A biological hybrid model for collagen-based tissue engineered vascular constructs. Biomaterials 2003 Mar;24(7):1241–54. [PubMed: 12527265]
3. Seliktar D, et al. Dynamic mechanical conditioning of collagen gel blood vessel constructs induces remodeling in vitro. Ann Biomed Eng 2000;28(4):351–62. [PubMed: 10870892]
4. Schmidt CE, Baier JM. Acellular vascular tissues: natural biomaterials for tissue repair and tissue engineering. Biomaterials 2000;21:2215–31. [PubMed: 11026628]
5. Schaner P, Martin N, Tulenko T, Shapiro I, Tarola N, Leichter R, et al. Decellularized vein as a potential scaffold for vascular tissue engineering. Journal of Vascular Surgery 2004;40( 1):146–53. [PubMed: 15218475]
6. Dahl SL, Koh J, Prabhakar V, Niklason LE. Decellularized native and engineered arterial scaffolds for transplantation. Cell Transplant 2003;12(6):659–66. [PubMed: 14579934]
7. Conklin BS, Richter ER, Kreutziger KL, Zhong DS, Chen C. Development and evaluation of a novel decellularized vascular xenograft. Med Eng Phys 2002 Apr;24(3):173–83. [PubMed: 12062176]
8. Ketchedjian A, Jones AL, Krueger P, Robinson E, Crouch K, Wolfinbarger L Jr, et al. Recellularization of decellularized allograft scaffolds in ovine great vessel reconstructions. Ann Thorac Surg 2005 Mar; 79(3):888–96. [PubMed: 15734400]discussion 96
9. Simionescu DT, Lu Q, Song Y, Lee JS, Rosenbalm TN, Kelley C, et al. Biocompatibility and remodeling potential of pure arterial elastin and collagen scaffolds. Biomaterials 2006 Feb;27(5):702–13. [PubMed: 16048731]
10. Rasmussen BL, Bruenger E, Sandberg LB. A new method for purification of mature elastin. Anal Biochem 1975 Mar;64(1):255–9. [PubMed: 1169889]
11. Vyavahare N, Jones PL, Tallapragada S, Levy RJ. Inhibition of matrix metalloproteinase activity attenuates tenascin-C production and calcification of implanted purified elastin in rats. Am J Pathol 2000 Sep;157(3):885–93. [PubMed: 10980128]
12. Bailey MT, Pillarisetti S, Xiao H, Vyavahare NR. Role of elastin in pathologic calcification of xenograft heart valves. J Biomed Mater Res A 2003 Jul 1;66(1):93–102. [PubMed: 12833435]
13. Lu Q, Ganesan K, Simionescu DT, Vyavahare NR. Novel porous aortic elastin and collagen scaffolds for tissue engineering. Biomaterials 2004 Oct;25(22):5227–37. [PubMed: 15110474]
14. Mithieux SM, Weiss AS. Elastin. Adv Protein Chem 2005;70:437–61. [PubMed: 15837523]

15. Eiken O. Autogenous connective tissue tubes for replacement of small artery defects. A preliminary report of an experimental study in dogs. Acta Chir Scand 1960 Nov 8;120:47–50. [PubMed: 13726126]

16. Schilling JA, Shurley HM, Joel W, Richter KM, White BN. Fibrocollagenous tubes structured in vivo. Morphology and biological characteristics. Arch Pathol 1961 May;71:548–53. [PubMed: 13747660]

17. Schilling JA, Shurley HM, Joel W, White BN, Bradford RH. Abdominal Aortic Grafts: Use of in Vivo Structured Autologous and Homologous Fibrocollagenous Tubes. Ann Surg 1964 Jun;159:819–28. [PubMed: 14170285]

18. Sparks CH. Autogenous grafts made to order. Ann Thorac Surg 1969 Aug;8(2):104–13. [PubMed: 5798828]

19. Sparks CH. Silicone mandril method for growing reinforced autogenous femoro-popliteal artery grafts in situ. Ann Surg 1973 Mar;177(3):293–300. [PubMed: 4266308]

20. Hallin RW, Sweetman WR. The Sparks' mandril graft. A seven year follow-up of mandril grafts placed by Charles H. Sparks and his associates. Am J Surg 1976 Aug;132(2):221–3. [PubMed: 133619]

21. Campbell JH, Efendy JL, Campbell GR. Novel vascular graft grown within recipient's own peritoneal cavity. Circ Res 1999 Dec 3–17;85(12):1173–8. [PubMed: 10590244]

22. Chue WL, Campbell GR, Caplice N, Muhammed A, Berry CL, Thomas AC, et al. Dog peritoneal and pleural cavities as bioreactors to grow autologous vascular grafts. J Vasc Surg 2004 Apr;39(4): 859–67. [PubMed: 15071455]

23. Li DY, Faury G, Taylor DG, Davis EC, Boyle WA, Mecham RP, et al. Novel arterial pathology in mice and humans hemizygous for elastin. J Clin Invest 1998 Nov 15;102(10):1783–7. [PubMed: 9819363]

24. Long J, Tranquillo R. Elastic fiber production in cardiovascular tissue equivalents. Matrix Biol 2003;22:339–50. [PubMed: 12935818]

25. Opitz F, Schenke-Layland K, Cohnert TU, Starcher B, Halbhuber KJ, Martin DP, et al. Tissue engineering of aortic tissue: dire consequence of suboptimal elastic fiber synthesis in vivo. Cardiovasc Res 2004 Sep 1;63(4):719–30. [PubMed: 15306228]

26. Nakayama Y, Ishibashi-Ueda H, Takamizawa K. In vivo tissue-engineered small-caliber arterial graft prosthesis consisting of autologous tissue (biotube). Cell Transplant 2004;13(4):439–49. [PubMed: 15468686]

27. Niklason LE, Gao J, Abbott WM, Hirschi KK, Houser S, Marini R, et al. Functional arteries grown in vitro. Science 1999 Apr 16;284(5413):489–93. [PubMed: 10205057]

28. Tieche C, Alkema PK, Liu SQ. Vascular elastic laminae: anti-inflammatory properties and potential applications to arterial reconstruction. Front Biosci 2004 Sep 1;9:2205–17. [PubMed: 15353282]

29. Carr SH, Zuckerman L, Caprini JA, Vagher JP. In vitro testing of surface thrombogenicity using the thrombelastograph. Res Commun Chem Pathol Pharmacol 1976 Mar;13(3):507–19. [PubMed: 935639]

30. Kidd KR, Nagle RB, Williams SK. Angiogenesis and neovascularization associated with extracellular matrix-modified porous implants. J Biomed Mater Res 2002 Feb;59(2):366–77. [PubMed: 11745574]

31. Gospodarowicz D. Fibroblast growth factor. Crit Rev Oncog 1989;1(1):1–26. [PubMed: 2484921]

32. Pepper MS, Ferrara N, Orci L, Montesano R. Potent synergism between vascular endothelial growth factor and basic fibroblast growth factor in the induction of angiogenesis in vitro. Biochem Biophys Res Commun 1992 Dec 15;189(2):824–31. [PubMed: 1281999]

33. PETERSON LH, JENSEN RE, PARNELL J. Mechanical Properties of Arteries in Vivo. Circulation Research 1960;8:622–39.

34. Stitzel J, Liu J, Lee SJ, Komura M, Berry J, Soker S, et al. Controlled fabrication of a biological vascular substitute. Biomaterials 2006 Mar;27(7):1088–94. [PubMed: 16131465]

35. Kobashi T, Matsuda T. Fabrication of compliant hybrid grafts supported with elastomeric meshes. Cell Transplant 1999 Sep–Oct;8(5):477–88. [PubMed: 10580342]

36. Girton TS, Oegema TR, Grassl ED, Isenberg BC, Tranquillo RT. Mechanisms of stiffening and strengthening in media-equivalents fabricated using glycation. J Biomech Eng 2000 Jun;122(3):216–23. [PubMed: 10923288]
37. Roeder R, Wolfe J, Lianakis N, Hinson T, Geddes LA. Burst pressure of canine carotid arteries. Australas Phys Eng Sci Med 2000 Jun;23(2):66–7. [PubMed: 10979597]
38. Hoenig MR, Campbell GR, Rolfe BE, Campbell JH. Tissue-engineered blood vessels: alternative to autologous grafts? Arterioscler Thromb Vasc Biol 2005 Jun;25(6):1128–34. [PubMed: 15705929]
39. Webb CL, Nguyen NM, Schoen FJ, Levy RJ. Calcification of allograft aortic wall in a rat subdermal model. Pathophysiology and inhibition by Al3+ and aminodiphosphonate preincubations. Am J Pathol 1992 Aug;141(2):487–96. [PubMed: 1497095]
40. Vyavahare N, Ogle M, Schoen FJ, Levy RJ. Elastin calcification and its prevention with aluminum chloride pretreatment. Am J Pathol 1999 Sep;155(3):973–82. [PubMed: 10487855]
41. Niederhoffer N, Lartaud-Idjouadiene I, Giummelly P, Duvivier C, Peslin R, Atkinson J. Calcification of medial elastic fibers and aortic elasticity. Hypertension 1997 Apr;29(4):999–1006. [PubMed: 9095090]
42. Hilbert SL, Boerboom LE, Livesey SA, Ferrans VJ. Explant pathology study of decellularized carotid artery vascular grafts. J Biomed Mater Res A 2004 May 1;69(2):197–204. [PubMed: 15057992]
43. Hinds MT, Courtman DW, Goodell T, Kwong M, Brant-Zawadzki H, Burke A, et al. Biocompatibility of a xenogenic elastin-based biomaterial in a murine implantation model: the role of aluminum chloride pretreatment. J Biomed Mater Res A 2004 Apr 1;69(1):55–64. [PubMed: 14999751]
44. Nauman EA, Sakata T, Keaveny TM, Halloran BP, Bikle DD. bFGF administration lowers the phosphate threshold for mineralization in bone marrow stromal cells. Calcif Tissue Int 2003 Aug;73 (2):147–52. [PubMed: 14565596]
45. Shiba H, Nakamura S, Shirakawa M, Nakanishi K, Okamoto H, Satakeda H, et al. Effects of basic fibroblast growth factor on proliferation, the expression of osteonectin (SPARC) and alkaline phosphatase, and calcification in cultures of human pulp cells. Dev Biol 1995 Aug;170(2):457–66. [PubMed: 7649376]
46. Varkey M, Kucharski C, Haque T, Sebald W, Uludag H. In vitro osteogenic response of rat bone marrow cells to bFGF and BMP-2 treatments. Clin Orthop Relat Res 2006 Feb;443:113–23. [PubMed: 16462434]
47. Naganawa T, Xiao L, Abogunde E, Sobue T, Kalajzic I, Sabbieti M, et al. In vivo and in vitro comparison of the effects of FGF-2 null and haplo-insufficiency on bone formation in mice. Biochem Biophys Res Commun 2006 Jan 13;339(2):490–8. [PubMed: 16298332]
48. Lee JS, Basalyga DM, Simionescu A, Isenburg JC, Simionescu DT, Vyavahare NR. Elastin calcification in the rat subdermal model is accompanied by up-regulation of degradative and osteogenic cellular responses. Am J Pathol 2006 Feb;168(2):490–8. [PubMed: 16436663]

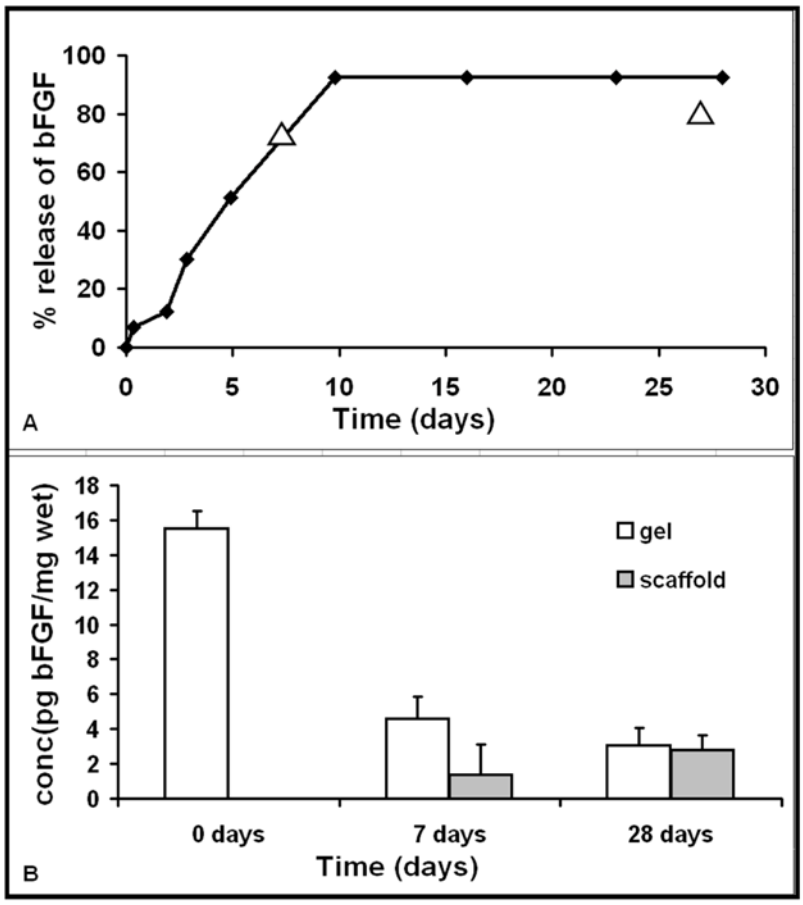


**Figure 1.**

*In vitro* release of bFGF from agarose gels **(A)** shows 70% release in 7 days. *In vivo* release of bFGF (shown as triangles) matches well with *in vitro* results. The total release in vitro was ~92% in 10 days. Fig 1(B) shows the gradual decrease of bFGF in the gel and a corresponding increase in the surrounding scaffold showing the sustained release through the gel and into the scaffold.

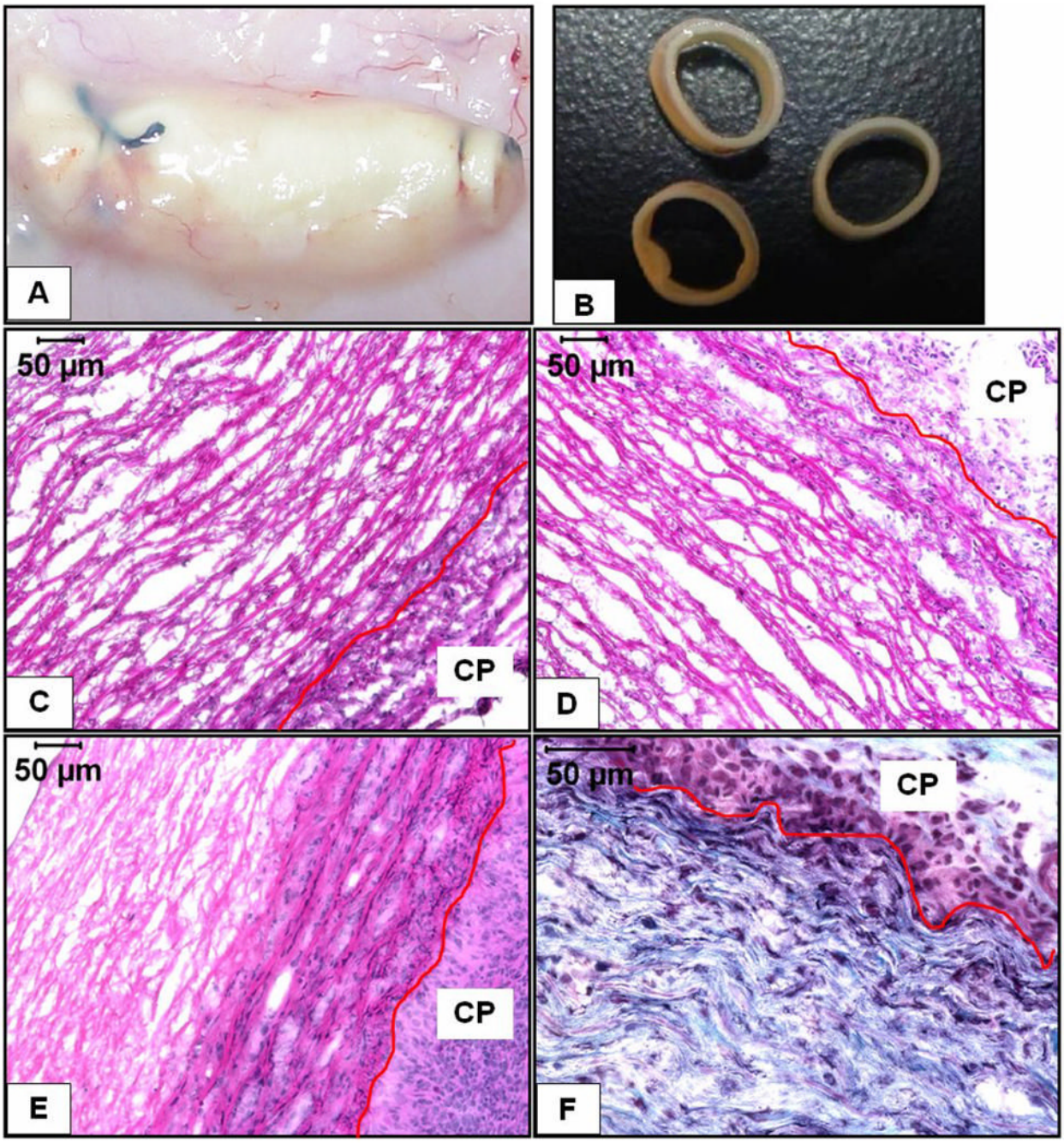


**Figure 2.**

Macroscopic and histological features of explanted EL scaffolds **(A)** shows the thin capsule over the explants **(B)** shows the structural integrity of the explants. 7d EL-Gel **(C)**, 7d EL-Gel-FGF **(D)** and 28d EL-Gel-FGF **(E)** representative images. Host cells could only infiltrate scaffolds by abluminal side. There is visibly reduced cell infiltration in EL-Gel group. Gomori's trichrome staining **(F)** shows new collagen fibers between layers of elastin only in the 28d EL-Gel-FGF group. The red lines indicate the scaffold-capsule interface. H&E stain (cell nuclei are dark blue and matrix is pink), Gomori's trichrome stain (cell nuclei are dark blue, collagen is blue – green and elastin is pink. Original magnifications (C –E) 200 X and (F) 400 X.

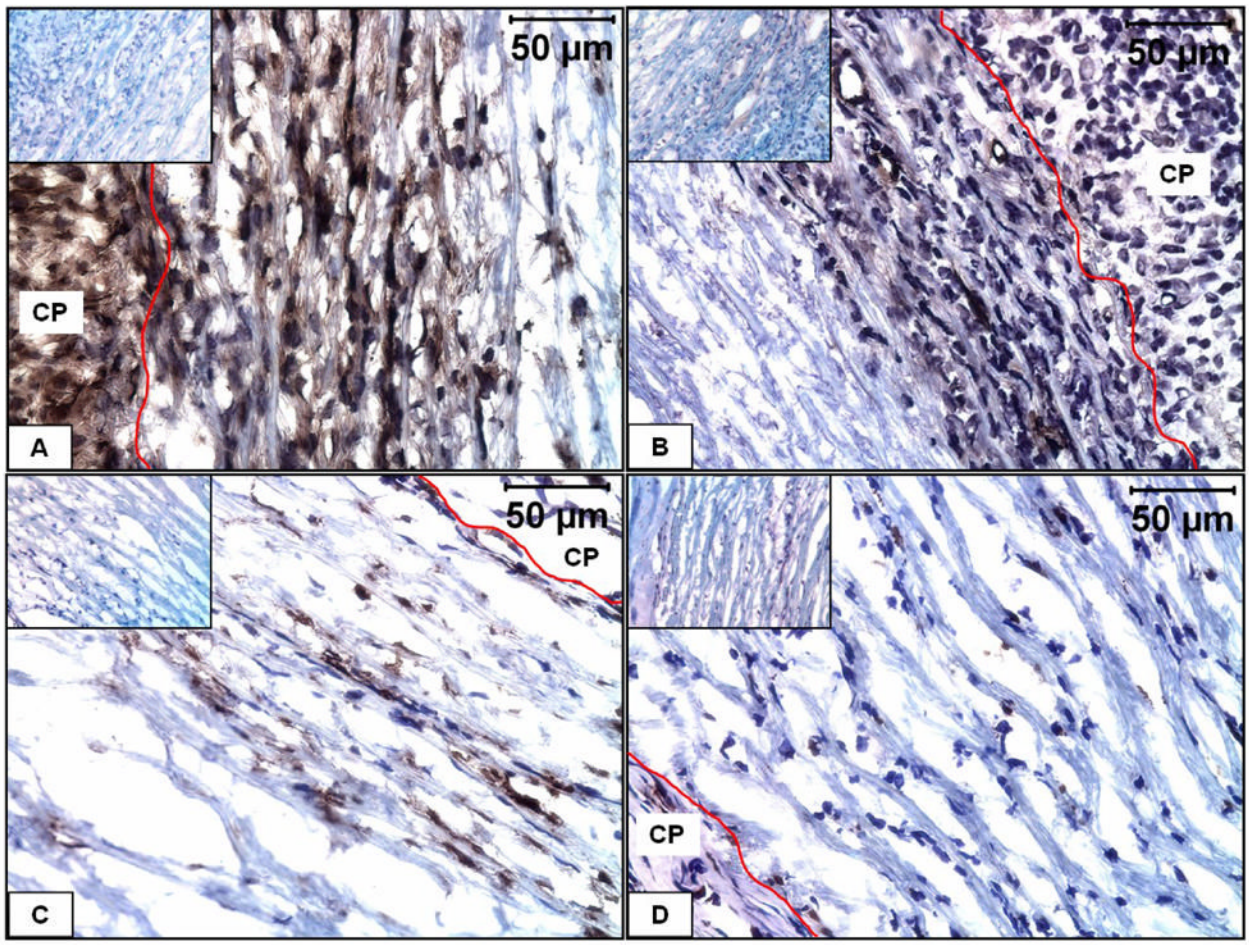


**Figure 3.**
Immunohistochemical characterization of infiltrating cells in EL-Gel-FGF scaffold. **A)** immunostained for fibroblasts at 28 day, **B)** immunostained for smooth muscle α-actin at 28 day, **C)** immunostaining for macrophages at 7 day, **D)** immunostaining for macrophages at 28 day. The red lines indicate the scaffold-capsule interface. Insets show negative stains. Original magnifications 400 X.

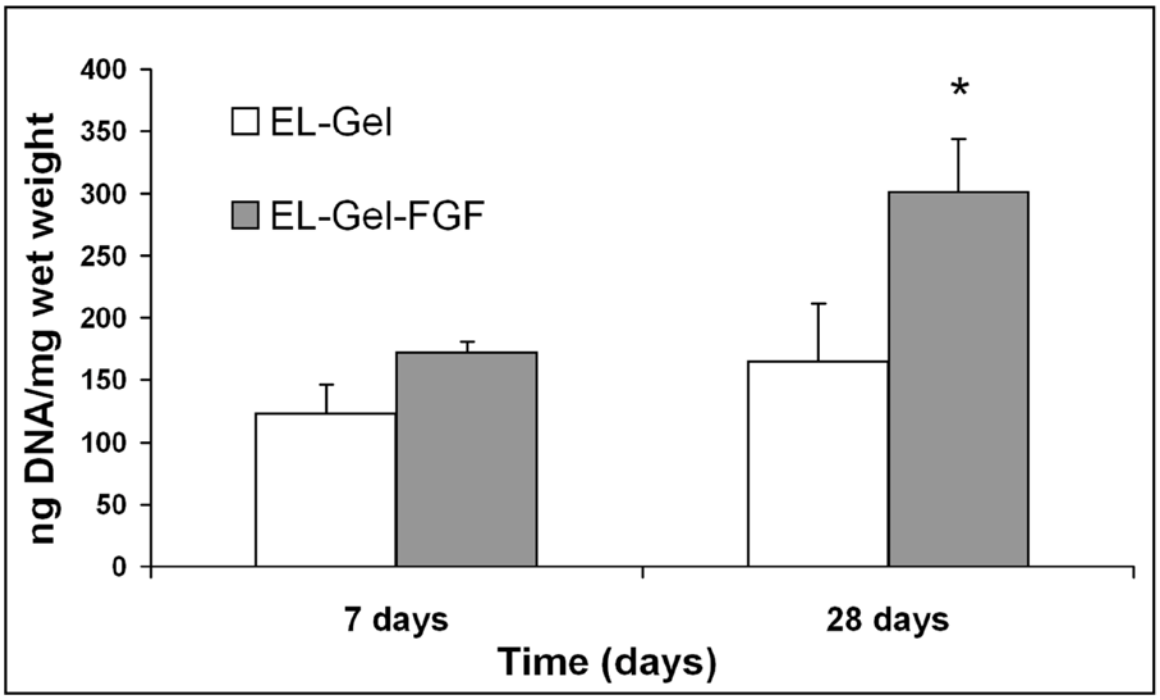


**Figure 4.**
Quantification of DNA within explanted scaffolds. At 28 days EL-Gel-FGF scaffolds had significantly more DNA ($p<0.05$)

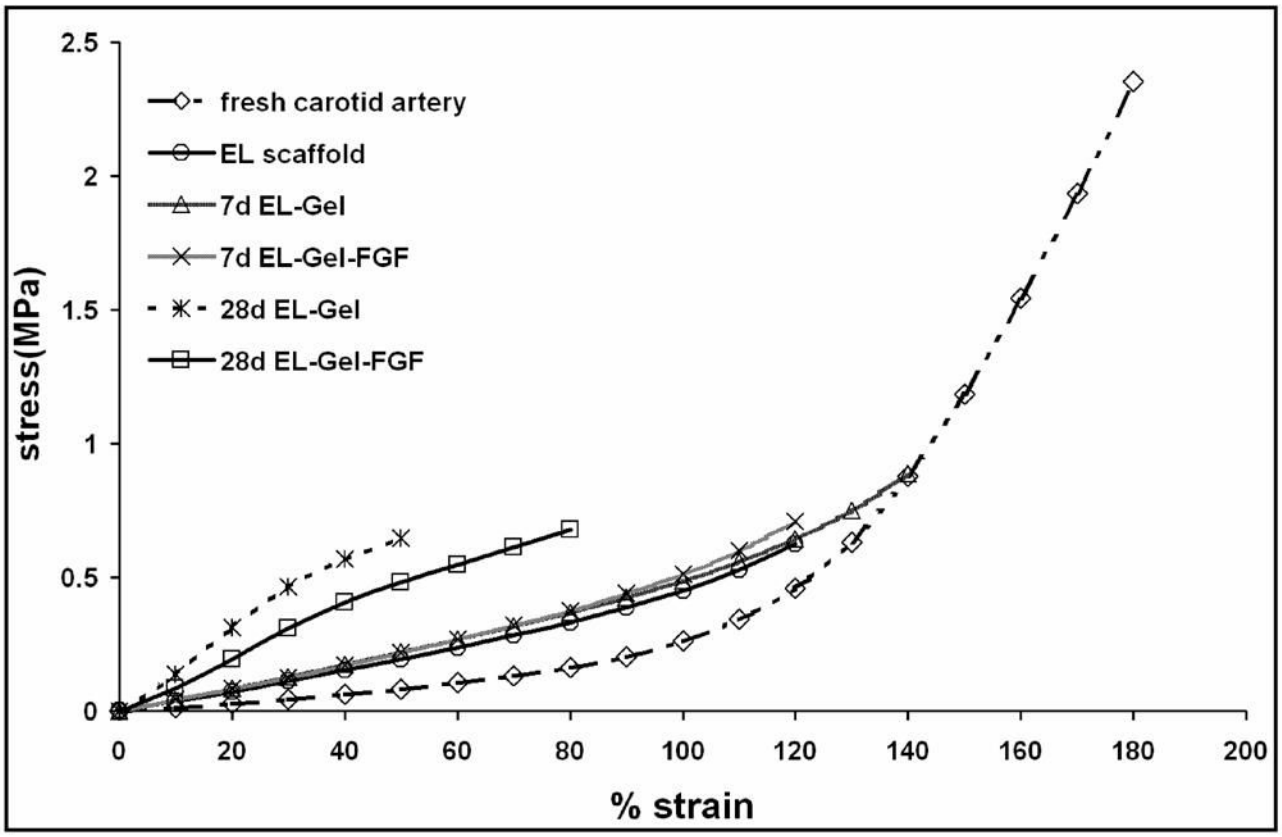


**Figure 5.**
Uniaxial tensile testing of fresh artery and scaffold rings. By 28 days, EL scaffolds were stiffer and less elastic.

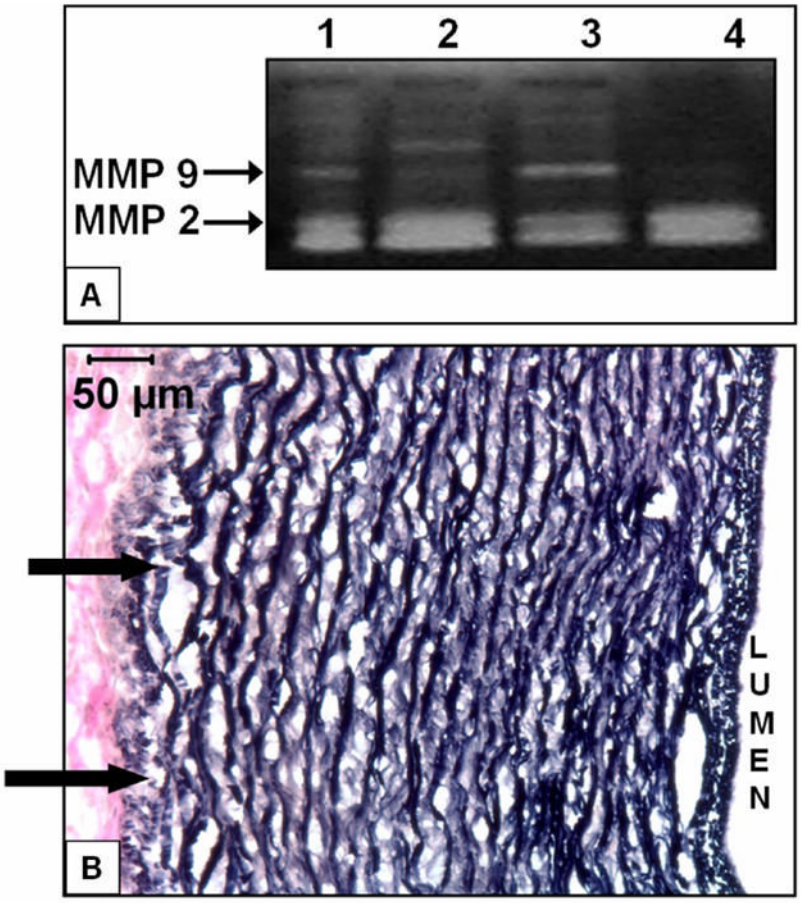


**Figure 6.**

Degradation of EL scaffolds *in vivo*. **A)** Gel image showing MMPs 2 and 9 in EL-Gel scaffolds 7day (Lane 1), EL-Gel scaffolds 28day (Lane 2), EL-Gel-FGF scaffolds 7day (Lane 3) and EL-Gel-FGF scaffolds 28day (Lane 4). **B)** VVG stain for elastic fibers. Arrows indicate degraded fibers on abluminal side (EL-Gel-FGF) at 28 days. Degradation was observed in both EL-Gel and EL-Gel-FGF samples at 28 days. Original magnification 200 X.

**Table I**

Depth of cellular infiltration into the scaffold. There was significantly more repopulation in the 28d EL-Gel-FGF scaffolds as compared to EL-Gel scaffolds ($p<0.01$).

| sample description | infiltration depth(μm) | tissue thickness(μm) | % infiltration depth | SEM |
|---|---|---|---|---|
| **7 day EL-Gel** | 9.74 | 218.58 | 4.46 | 0.93 |
| **7 day EL-Gel-FGF** | 27.48 | 212.96 | 12.91 | 2.91 |
| **28 day EL-Gel** | 41.92 | 243.32 | 17.23 | 1.86 |
| **28 day EL-Gel-FGF** | 107.43 | 235.66 | 45.59 | 1.98 |

**Table II**

Mechanical properties of pre-implant and explanted scaffolds. Values are averages of 6 samples ± SEM

| | fresh carotid | EL scaffold | 7d EL-Gel | 7d EL-Gel-FGF | 28d EL-Gel | 28d EL-Gel-FGF |
|---|---|---|---|---|---|---|
| **avg ultimate stress (MPa)** | 1.97 ± 0.08 | 0.69 ± 0.04 | 0.95 ± 0.06 | 0.76 ± 0.11 | 0.57 ± 0.04 | 0.55 ± 0.08 |
| **avg ultimate %strain** | 158.33 ± 10.78 | 121.67 ± 4.77 | 160 ± 10.65 | 115 ± 12.32 | 51.67 ± 5.43 | 50 ± 10.33 |
| **elastic modulus (MPa)** | 0.16 ± 0.007 | 0.39 ± 0.01 | 0.41 ± 0.03 | 0.46 ± 0.04 | 1.49 ± 0.21 | 1.44 ± 0.48 |